RNase1 Prevents the Damaging Interplay between Extracellular RNA and Tumor-Necrosis-Factor-α in Cardiac Ischemia/Reperfusion Injury

H. A. Cabrera-Fuentes[1,5], M. Ruiz-Meana[6†], S. Simsekyilmaz[7†], S. Kostin[8†], J. Inserte[6], M. Saffarzadeh[1], G. Barreto[9], S. P. Galuska[1], V. Vijayan[3], I. Barba[6], S. Pedretti[10], T. Adam[10], G. Lochnit[1], O. N. Ilinskaya[5], E. Baumgart-Vogt[3], S. Fischer[1], S. Lecour[10], A. Böning[4], D. J. Hausenloy[11], E. A. Liehn[7], D. Garcia-Dorado[6], K. D. Schlüter[2], K. T. Preissner[1*]

[1]Institute of Biochemistry, [2]Institute of Physiology, [3]Institute of Anatomy and Cell Biology II, [4]Department of Cardiovascular Surgery, Medical School, Justus-Liebig-University, Giessen, Germany;

[5]Kazan Federal University, Department of Microbiology, Kazan, Russian Federation;

[6]Hospital Universitari Vall d´Hebron, Laboratorio de Cardiología Experimental, Barcelona, Spain;

[7]Institute of Molecular Cardiovascular Research, RWTH, Aachen, Germany.

[8]Core Lab for Molecular and Structural Biology, [9]LOEWE Research Group Lung Cancer Epigenetics, Max-Planck-Institute, Bad Nauheim, Germany;

[10]Hatter Institute for Cardiovascular Research, University of Cape Town, Cape Town, South Africa;

[11]The Hatter Cardiovascular Institute, University College London, London, United Kingdom.

† = Equal contributions

***Correspondence address:**

Klaus T. Preissner, PhD
Depart. Biochemistry, Medical School
Justus-Liebig-Universität
Friedrichstrasse 24
35392 Giessen, Germany
Tel. +49-641-994-7500; Fax. +49-641-994-7509
e-mail: klaus.t.preissner@biochemie.med.uni-giessen.de

Abstract

Despite optimal therapy, the morbidity and mortality of patients presenting with an acute myocardial infarction (MI) remain significant, and the initial mechanistic trigger of myocardial "ischemia/reperfusion (I/R) injury" remains greatly unexplained. Here we show that factors released from the damaged cardiac tissue itself, in particular extracellular RNA (eRNA) and tumor-necrosis-factor α (TNF-α), may dictate I/R injury. In an experimental *in vivo* mice model of myocardial I/R as well as in the isolated I/R Langendorff-perfused rat heart, cardiomyocyte death was induced by eRNA and TNF-α. Moreover, TNF-α promoted further eRNA release especially under hypoxia, feeding a vicious cell damaging cycle during I/R with the massive production of oxygen radicals, mitochondrial obstruction, decrease in antioxidant enzymes and decline of cardiomyocyte functions. The administration of RNase1 significantly decreased myocardial infarction in both experimental models. This regimen allowed the reduction in cytokine release, normalization of antioxidant enzymes as well as preservation of cardiac tissue. Thus, RNase1 administration provides a novel therapeutic regimen to interfere with the adverse eRNA-TNF-α interplay and significantly reduces or prevents the pathological outcome of ischemic heart disease.

Introduction

Cardiomyocyte death occurring during acute myocardial infarction has a significant impact on the quality of life and survival of patients suffering from coronary artery disease, the most eminent single cause of death worldwide (1). Severe myocardial ischemia secondary to a thrombotic coronary occlusion at the site of a ruptured atheromatous plaque results in an extensive cardiomyocyte death involving most of the area at risk unless coronary blood flow is rapidly restored by pharmacological or mechanical interventions (2). However, although early reperfusion salvages viable myocardium, limits infarct size and markedly improves the prognosis of patients with acute myocardial infarction, its beneficial effect is limited by the occurrence of additional cardiomyocyte death during the initial minutes of reflow, a phenomenon described as lethal ischemia/reperfusion (I/R) injury (3).

This paradoxical phenomenon has largely been studied in experimental animal models and is known to be caused by a network of mechanisms causing Ca^{2+}-overload (4), mitochondrial permeabilization (5, 6) or ATP-dependent hyper-contracture (7, 8) that may limit myocardial salvage achieved by reperfusion (9). Experimental studies have convincingly demonstrated that infarct size can be markedly reduced by therapeutic interventions applied at the time of reperfusion, such as ischemic post-conditioning (10), and diverse pharmacological interventions aimed to improve intracellular calcium handling. Moreover, heart protection was experimentally achieved by reduction of hyper-contracture and mitochondrial permeability transition (11), modulation of Na^+/H^+ ion exchanger (12) or application of particulate guanylyl-cyclase agonist (13): However, none of the mentioned cardio-protective approaches has been demonstrated to improve patients' outcome. Nevertheless, non-invasive intermittent limb I/R (designated as remote ischemic preconditioning), applied either prior to heart operation (14, 15) or upon primary percutaneous coronary intervention (PPCI) to patients with ST-Segment elevation myocardial infarction (STEMI) (16), has been successfully employed (17, 18) and may become introduced into clinical practice.

Experimental studies thus far have not taken into account that factors released from the damaged cardiac tissue itself may have detrimental effects on reperfused cardiomyocytes and contribute to lethal reperfusion injury and final infarct size. Although it is well known that disrupted cells may release cytosolic proteins during reperfusion, such as creatine kinase or cardiac troponins, these and other factors have only been used for diagnostic evaluation (19, 20). Other components that are detectable in the extracellular space during tissue hypoxia or cell damage are ribonucleic acids (RNA), which are released by damaged cells and designated as extracellular RNA (eRNA) (21). Based on our former work, the majority of eRNA consists of ribosomal RNA, which binds to different basic proteins in blood plasma or on cell surfaces, and thereby promotes a variety of extracellular functions, particularly related to vascular diseases (22, 23). These include activation of blood coagulation / thrombosis, release of TNF-α and other cytokines as well as promotion of inflammatory processes, such as leukocyte trafficking (24).

Here, we demonstrate an obligate role for eRNA and TNF-α as early alarm signals in cardiac tissue damage that determine the cell fate during cardiac I/R. Consequently, in the current study, we demonstrate that the administration of ribonuclease1 (RNase1) to inhibit eRNA reduced pathological parameters that are characteristic of I/R injury and substantially improved the early post-ischemic functional myocardial recovery.

Materials and Methods

Extracellular RNA (eRNA) quantification

eRNA was quantified in mice plasma, in the perfusate obtained from the isolated Langendorff heart using the Master Pure^{TM} RNA Purification kit (Epicentre Biotechnologies). Total RNA concentration was quantified with NanoDrop ND-2000 (peqLab Biotechnologie GmbH).

Microparticle isolation

Langendorff-perfusate (1 ml) was collected at each time point and fractions were combined to perform ultracentrifugation for isolation of microparticles as described (25). To analyse the quality of microparticle-associated RNA, the above-mentioned purification procedure was used.

Treatment with RNase 1 or RNase-inhibitor (RI) after induction of ischemia-reperfusion (I/R) in mice.

The established *in vivo* experimentation was exactly carried out as previously described (26). Animals were treated with a continuous treatment (started three days before surgery) of RNase1 (Fermentas®, 100 µg/mouse) or RNase Inhibitor (RiboLock, Fermentas®, 80 U/mouse) via a subcutaneously implanted miniature infusion Alzet® osmotic pump (model 1004). Quantification of the infarcted area and *in vivo* assessments of cardiac functions were done as described (26). All animal experiments and study protocols were approved by local authorities of the RWTH Aachen, complying with Romanian and German animal protection laws. Animals were housed and treated in accordance with the Guide for Care and Use of Laboratory Animals (Eighth Edition), published by the US National Institute of Health Publications.

Langendorff heart perfusion system

Wistar rats (10-12 weeks old; weighing 225–300 g) were specific pathogen free, and kept at the animal care facility, Justus-Liebig-University, Giessen, with free access to food and water, conforming to the Guide for the Care and Use of Laboratory Animals, National Institute of Health (NIH publication no. 85-23, revised 1996). Experiments were performed on isolated hearts as previously described (27); experimental conditions are outlined in the corresponding legends to Figures.

Quantification of cell death

Lactate dehydrogenase (LDH) activity in the Langendorff-perfusate was measured during the entire reperfusion period of 120 min by a detection kit (Roche Diagnostics) (28). Thereafter, hearts were cut into four slices and incubated at 37°C for 10 min in 1% triphenyltetrazolium chloride (pH 7.4) and imaged under white light to outline the area of necrosis (29).

ROS immunolabeling and fluorescent microscopy

Mice hearts from *in vivo* experiments or rat hearts from the different experimental groups were removed from the Langendorff system, weighed and rapidly frozen in liquid nitrogen. *In situ* reactive oxygen species (ROS) were determined by labelling with dihydroethidium as described (30).

Quantification of TNF-α

Mice plasma from *in vivo* experiments and Langendorff heart-perfusates were collected and filtered through 0.2 μm filter to remove any residual debris and used for subsequent quantification of TNF-α as described. TNF-α production by heart tissue submitted to I/R was assessed by enzyme-linked immune-sorbent assay (ELISA) (Quantikine®**,** R&D Systems) according to manufacturer's protocol. Absorbance values for individual reactions were determined using VersaMax™ Microplate Reader with SoftmaxPro 3.0 data processing

software.

RNA isolation and quantitative Real Time PCR analysis (qRT-PCR)

DNA-free total RNA was extracted from homogenised heart tissue using *TRIzol® Reagent (Invitrogen, USA*). Standard procedures were used for qRT-PCR **(Table 1)**.

Statistics

Data were analyzed by paired and unpaired Student's t test or One-way ANOVA analysis of variance followed by Tukey's, Dunnett's or Bonferroni's multiple comparisons test was performed, when appropriate, to determine statistical significance of the differences using GraphPad Prism version 6.00 for Mac OS X, GraphPad Software, La Jolla California U.S.A. (www.graphpad.com). Significance values are *P<0.05, **P<0.01, ***P<0.001 and ns for non-significant (p>0.05).

Results

Extracellular RNA (eRNA) promotes I/R injury and myocardial infarction.

In order to prove the release of eRNA upon ischemic heart disease, a myocardial infarction model in mice and the isolated rat Langendorff heart model, exposed to I/R injury, were investigated. Following coronary artery ligation in mice for 60 min, eRNA levels were significantly elevated during the subsequent 120 min reperfusion phase **(Fig. 1A)**. The sham group did not show any changes on eRNA levels during the course of the experiment (data not shown). In order to delineate the cellular origin of eRNA, RT-PCR analysis was carried out to amplify cell-specific mRNA that was found associated with the released 18S/28S rRNA **(Fig. 1B, insert)**. Results indicate that eRNA is derived mainly from cardiomyocytes (expressing SERCA) (31) and to a much lesser degree from smooth muscle cells (32) (expressing α-smooth muscle actin), myofibroblasts (expressing bHLH transcription factor - *Tcf21*) *(33)* and endothelial cells, expressing CD31 **(Fig. 1B)**.

After excision and perfusion equilibration of isolated rat hearts connected to the Langendorff apparatus, blood-free perfusion was arrested for 45 min to achieve global ischemia and thereafter, reperfusion was resumed for 120 min. At the start of the reperfusion phase, a significant increase in eluted eRNA was observed **(Fig. 1C)**, together with other markers of myocardial injury such as lactate dehydrogenase (LDH), cardiac troponins and creatine kinase (34) (data not shown). In contrast to the latter parameters, a second washout peak of eRNA during reperfusion between 15 and 60 min was noted that related to more than 60% of the totally recovered eRNA. Analysis of eRNA collected from the entire 120 min reperfusion phase revealed a significant portion of microparticle-associated eRNA **(Fig. 1C, insert)**.

Hypoxia and eRNA promote cardiac I/R-induced TNF-α release.

Since we had previously observed a close relationship between the appearance of eRNA and TNF-α in situations of chronic inflammation (32, 35, 36) the indicated experimental models were used to define the conditions of I/R injury under which TNF-α release may occur. While in the murine heart ligation model under constant (normoxic) perfusion – sham; no significant TNF-α liberation was observed in the animal circulation **(Fig. 2A)** as well as in heart tissue **(Fig. 2B)**, exposure to ischemia for 60 min, followed by various time intervals of reperfusion (0, 2 and 120 min) all resulted in massive increase in TNF-α release with I/R of 60 min/2 min showing the highest value (>20 fold) **(Fig. 2A)**. Likewise, these conditions were associated also with a dramatic appearance of TNF-α in heart tissue of these animals **(Fig. 2B)**. While the administration of RNase1 resulted in a drastic reduction of TNF-α release and tissue deposition, the application of an RNase inhibitor (RI) had no significant influence on the eRNA/hypoxia-induced liberation of TNF-α.

Upon I/R exposure in isolated rat hearts, significantly increased levels of TNF-α were detectable in the perfusate during the initial 15 min reperfusion phase in accordance with a report in which the gene for this cytokine was found to be transcribed during this I/R phase (37). Treatment with RNase1 reduced the level of TNF-α almost to background values **(Fig. 2C)**, while after 120 min reperfusion, TNF-α mRNA was significantly decreased in the RNase1 treatment group **(Fig. S1)**. In contrast, administration of RI had neither an influence on liberation of TNF-α nor on its mRNA expression when compared to the I/R group **(Fig. 2C** and **Fig. S1)**.

Production of reactive oxygen species (ROS) during I/R injury and prevention by RNase1.

The production of ROS during ischemic heart disease is a causally-related hall-mark in the pathogenesis of myocardial infarction, playing a significant role in damaging the heart during I/R (38, 39). Upon exposure of mice to 60 min regional ischemia (by coronary artery ligation),

followed by different time intervals of reperfusion, inspection of heart tissue by confocal microscopy revealed a markedly disturbed cardiomyocyte structure, accompanied by a significant elevation of ROS, which were found at intra-nuclear sites overlapping with the DAPI stain for condensed DNA, as documented in **Fig. 3A**. The same was true when tissue samples from the isolated Langendorff rat heart model, under conditions of 45 min ischemia and various reperfusion intervals, were inspected **(Fig. 3B)**. In contrast, in RNase1-treated mice or isolated rat hearts, not only was the tissue architecture greatly preserved, but the fluorescence intensity of ROS was low, similar to control sections, not exposed to I/R. ROS content in cardiac tissue (mice: 199 ± 15 AU/μm^2, isolated rat hearts: 209 ± 11 AU/μm^2) following I/R was reduced upon RNase1 treatment to 88 ± 20 AU/μm^2 in mice and 70 ± 12 AU/μm^2 in isolated rat hearts ($P<0.001$ for each case). As expected, RI treatment did not prevent tissue destruction, and ROS accumulation was as extensive as in the non-treated I/R injury groups.

To further substantiate the influence of anti-oxidant enzymes in cardiomyocytes on ROS production, RT-PCR analysis of peroxiredoxin 3 and isoforms of superoxide dismutase (SOD), representing cytoplasmic SOD1, mitochondrial SOD2 and extracellular SOD3, was performed in the Langendorff heart model, exposed to the ischemia-related protocols. While low mRNA levels of these antioxidant enzymes were found in the isolated heart after 120 min reperfusion only, administration of RNase1 in isolated hearts submitted to I/R resulted in significantly elevated mRNA levels of these enzymes, particularly peroxiredoxin 3 and SOD 2 **(Fig. S2)**.

RNase1 protects against cardiac I/R injury and reduces infarct size.

Following induction of acute cardiac I/R injury in the mouse model, infarct size expressed as the percentage of the area of risk was smaller in hearts administered with RNase1 when compared to those administrated with buffer alone or RI, respectively **(Fig. 4A, Fig. S3)**,

indicative for the causal contribution of eRNA to cardiac tissue damage. Likewise, mice, treated with vehicle for 14 days following reperfusion, developed myocardial infarcts comparable to the RI-treated group (16 ± 3% vs. 15 ± 2%), whereas the RNase1 treatment group (3 ± 1%) was protected against cardiac tissue injury and developed significantly smaller infarcts **(Fig. 4B)**. Intra-ventricular measurements at day 14 after I/R revealed a significant decrease in left ventricular developed pressure, contraction and relaxation in the sham and RI-treated groups, whereas the RNase1-treated group exhibited preserved heart function comparable with sham or non-injured mice **(Fig. S4 A-C)**. As shown in Fig. 4B, continuous administration of RNase1 or RNase-inhibitor during the 14 days course of the experimental model did not create any adverse effects in the animals.

To characterize the beneficial effects of RNase1 upon myocardial parameters in the Langendorff heart model under I/R conditions, three groups receiving increasing concentrations of RNase1 as well as one RI-group were studied. The drugs were administered together with the perfusion buffer prior to the induction of 45 min ischemia **(Fig. S5A)**. Assessment of left ventricular end-diastolic pressure (LVEDP, a measure of the magnitude of ischemic rigor contracture) in the RI-group (34 ± 5 mmHg) revealed a similar or even higher value when compared to non-treated I/R hearts (26 ± 4 mmHg), whereas RNase1 in a concentration-dependent manner significantly reduced the adverse outcome of I/R (11 ± 3 mmHg at 10 µg/ml) and was effective over the entire reperfusion phase **(Fig. S5B)**. Similarly, cardiomyocyte hypercontracture (a measure of I/R-mediated injury) was significantly reduced in the RNase1-treated groups (30 ± 4 mmHg at 10 µg/ml), while RI-administration (104 ± 8 mmHg) resulted in an even worse (although not significant) effect when compared to the untreated I/R group (66 ± 9 mmHg) **(Fig. S5C)**.

Furthermore, only minor quantities of LDH were detectable in all perfusate fractions in the RNase1 treatment groups, indicating markedly reduced necrotic cell death, whereas the typical early release of LDH following reperfusion was documented in both, the buffer and RI-

treated groups subjected to I/R **(Fig. 4C)**. The cumulative LDH release was markedly reduced in the RNase1 group (44 ± 7 UI/g tissue, *vs.* 127 ± 32 UI/g tissue in I/R group) (**Fig. S5D)**. Most importantly, RNase1-administration substantially decreased infarct size in the isolated heart (23% *vs.* 66 ± 5%, P<0.001) **(Fig. 4D)**, while the application of RI had no effect on these parameters when compared to I/R injury alone. Likewise, in the RNase1 treatment group, contractile recovery (expressed as left ventricular developed pressure, LVdevP) was significantly improved (73 ± 13% of basal values, *vs.* 38 ± 12% of basal values in I/R group) after 120 min reperfusion **(Fig. S5E)**. Ischemia in the isolated rat heart induced a rapid exhaustion of phosphocreatine as a quantity of energy depletion with only partial recovery in the control I/R group (45 ± 5%) after 15 min of reperfusion, whereas in the RNase1 treatment group intracellular phosphocreatine remained elevated at a significantly higher level (73 ± 5%, P=0.032) and promoted substantial heart recovery **(Fig. S5F)**. Finally, we reasoned that the beneficial RNase1-treatment might be due to the generation of certain RNA degradation products such as nucleotides or nulceosides like adenosine (40, 41). The adenosine-receptor antagonist 8-sulfophenyltheophylline (8SPT) was tested in the Langendorff system, but did not influence the infarct size-reducing effect of RNase1, and 8SPT alone did not affect the control infarct size **(Fig. S6)**.

Discussion

In the present study, novel mechanistic insights into the process of cardiac I/R injury that are governed by the endogenous extracellular RNA/RNase system were obtained. Moreover, the indicated interplay between eRNA-dependent and TNF-α-related pathomechanisms (H.A. Cabrera-Fuentes, et al., 2014; unpublished data) may not be limited to ischemic heart disease but may be applied generally to ischemia-mediated damage of other organs or tissues as well, such that interventions with RNase1 would definitely provide a new regimen for cytoprotection in general.

The rationale for studying the role of eRNA in ischemic heart disease was based upon our previous findings that these poly-anionic compounds promoted arterial thrombosis (21), induced the release of cytokines (including TNF-α), and served to elevate vascular permeability and edema formation *in vivo* (42). Collectively, these functional activities of eRNA were largely inhibited by RNase1, which thereby plays a prominent role as a vessel-and tissue-protective agent (43). Moreover, in cardiac patients undergoing cardiac bypass surgery, in which the heart is subjected to IRI, significantly elevated levels of eRNA (>20 fold) and TNF- α (>7-fold) were found, especially in coronary sinus blood before unclamping as compared to peripheral arterial blood (data not shown).

Acutely elevated levels of eRNA, both free and in association with micro-particles, were found upon onset of reperfusion in the isolated rat heart model in accordance with a recent report demonstrating the release of tissue factor-bearing micro-particles from cardiomoycytes under inflammatory conditions (35, 44). Likewise, in acute models of vessel stenosis or chronic models of atherosclerosis in mice, we observed increased plasma and tissue concentrations of eRNA (32). In the Langendorff heart model, the initial reperfusion-dependent washout of eRNA together with cardiomyocyte-specific markers such as creatine kinase or troponins was followed by a second peak of eRNA, whereby the vast majority of this 18S/28S rRNA material

was derived from cardiomyocytes. Thus, unlike creatine kinase, troponins or LDH, eRNA remains to be released into the perfusate over an appreciable period of time where it can directly or indirectly affect cellular functions.

Moreover, in the *in vivo* as well as in the *ex vivo* cardiac I/R injury model, substantial amounts of TNF-α were released and became deposited in cardiac tissue, whereas these TNF-α values remained almost at control level in the presence of RNase1. Collectively, these findings support our contention of an eRNA-promoted liberation of TNF-α and its reciprocal amplification in a positive feedback mechanism, particularly under conditions of I/R injury, with the result of generating appreciable amounts of the cytokine (32, 35, 36).

ROS are another group of major inducers of cellular damage under conditions of cardiac I/R injury, and their prominent contribution to organ damage is without doubt. Yet, the causal molecular relations that would lead to massive ROS generation under pathological conditions are incompletely understood. Here, we present strong evidence, both in the *in vivo* and *ex vivo* experimental models, that the elevation of ROS in plasma or perfusate as well as in association with the damaged myocardium were substantially reduced or prevented by RNase1. Thus, it is concluded that the proposed eRNA-TNF-α interplay provides a major stimulus for ROS production and deposition. Mechanistically, in combination with hypoxia/ischemia, eRNA provoked a marked reduction in the expression of antioxidant enzymes, indicative of the fact that such endogenous protective factors become down-regulated under stress conditions. RNase1 could reverse this effect by inducing the expression of such enzymes like peroxiredoxin 3 or the three isoforms of SOD in the Langendorff heart model. In addition, RNase1 reduced the expression of iNOS and MCP-1, factors which are known to be involved in mediating cell-damaging signals in cardiomyocytes. Together, these data strongly imply that the imbalance of the eRNA/RNase1 system culminates in ROS production and cardiomyocyte death and that RNase1 serves a potent cardio-protective function.

In support of this contention, administration of RNase1 resulted in markedly reduced contractility and left ventricular end-diastolic pressure (as a measure of the magnitude of rigor contracture) of the heart, as well as in very low levels of LDH in the perfusate as a general marker for necrotic cell death. Together with the massive reduction of ROS in cardiomyocytes as well as the preservation of tissue architecture, the multitude of physiological parameters that were protected by application of RNase1 provide compelling evidence for its causative relation to tissue protection. Although it is tempting to assume that the beneficial effects of RNase1 treatment may depend on certain RNA degradation products such as adenosine (40, 41), we found no evidence for this relation **(Fig. S6).**

Also, it should not be ignored that low doses of TNF-α may contribute to ischemic preconditioning protection by a direct effect on mitochondria (45-47). In contrast to intervention with antibodies against TNF-α that would capture the entire pool of the cytokine and may induce adverse effects (48), the treatments with RNase1 in this study prevented excessive TNF-α production, but may have left sufficient quantities of the cytokine, to promote protective functions via TNF-receptor-2 signalling (49).

Finally, the overall measure of organ damage in cardiac I/R injury is ultimately quantitated by the degree of cell death and the respective infarct size. Here, RNase1 not only significantly prevented LDH-release, but expressed a robust protective effect in tissue recovery as demonstrated in the acute or chronic *in vivo* disease model or the *ex vivo* Langendorff system. The protective treatment with RNase1 in any of these experimental models appears to be maximal, provided the time-point of intervention during the I/R situation is chosen as early as possible, preferentially before or during the ischemic phase. This will determine the overall outcome of I/R injury with respect to ROS generation, cytokine release, macrophage polarization not only for the acute endpoint. The beneficial outcome of RNase1 treatment is largely diminished, if the intervention was started after the onset of reperfusion or later (data not shown). This indicates that counteracting the damaging factors/reactions during the critical

ischemic phase will have a major impact on the outcome of the therapeutic maneuver, possibly also for a long-range endpoint. Moreover, further beneficial outcome is expected under long-term administration of RNase1, since eRNA may become released from the damaged tissue over a longer time period, as was recently shown in an atherosclerotic mouse model, where continuous infusion of RNase1 over three weeks resulted in a significant reduction of neointima formation (32).

Thus, RNase1 appears to be an evidenced-based new protective drug to limit cardiac infarct size, dependent on the here presented pathogenetic mechanism. In addition, during coronary vessel canalization these drugs may be administered alone or together with a stent-operating procedure to significantly reduce or prevent the pathological outcome of ischemic heart injury. This newly uncovered fundamental pathomechanism is likely to be operative in other organs and tissues as well.

References

1. Yellon DM, Hausenloy DJ. Myocardial reperfusion injury. The New England journal of medicine 2007; 357(11): 1121-35.
2. Hausenloy DJ, Yellon DM. Myocardial ischemia-reperfusion injury: a neglected therapeutic target. The Journal of clinical investigation 2013; 123(1): 92-100.
3. Piper HM, Garcia-Dorado D, Ovize M. A fresh look at reperfusion injury. Cardiovascular research 1998; 38(2): 291-300.
4. Ruiz-Meana M, Abellan A, Miro-Casas E, et al. Opening of mitochondrial permeability transition pore induces hypercontracture in Ca2+ overloaded cardiac myocytes. Basic research in cardiology 2007; 102(6): 542-52.
5. Di Lisa F, Carpi A, Giorgio V, et al. The mitochondrial permeability transition pore and cyclophilin D in cardioprotection. Biochimica et biophysica acta 2011; 1813(7): 1316-22.
6. Di Lisa F, Kaludercic N, Carpi A, et al. Mitochondria and vascular pathology. Pharmacological reports : PR 2009; 61(1): 123-30.
7. Abdallah Y, Wolf C, Meuter K, et al. Preconditioning with diazoxide prevents reoxygenation-induced rigor-type hypercontracture. Journal of molecular and cellular cardiology 2010; 48(1): 270-6.
8. Ladilov Y, Efe O, Schafer C, et al. Reoxygenation-induced rigor-type contracture. Journal of molecular and cellular cardiology 2003; 35(12): 1481-90.
9. Garcia-Dorado D, Ruiz-Meana M, Inserte J, et al. Calcium-mediated cell death during myocardial reperfusion. Cardiovascular research 2012; 94(2): 168-80.
10. Zhao Q, Shao L, Hu X, et al. Lipoxin a4 preconditioning and postconditioning protect myocardial ischemia/reperfusion injury in rats. Mediators of inflammation 2013; 2013: 231351.
11. Schafer C, Ladilov Y, Inserte J, et al. Role of the reverse mode of the Na+/Ca2+ exchanger in reoxygenation-induced cardiomyocyte injury. Cardiovascular research 2001; 51(2): 241-50.
12. Ruiz-Meana M, Garcia-Dorado D, Julia M, et al. Protective effect of HOE642, a selective blocker of Na+-H+ exchange, against the development of rigor contracture in rat ventricular myocytes. Experimental physiology 2000; 85(1): 17-25.
13. Agullo L, Garcia-Dorado D, Escalona N, et al. Membrane association of nitric oxide-sensitive guanylyl cyclase in cardiomyocytes. Cardiovascular research 2005; 68(1): 65-74.
14. Hausenloy DJ, Mwamure PK, Venugopal V, et al. Effect of remote ischaemic preconditioning on myocardial injury in patients undergoing coronary artery bypass graft surgery: a randomised controlled trial. Lancet 2007; 370(9587): 575-9.
15. Thielmann M, Kottenberg E, Kleinbongard P, et al. Cardioprotective and prognostic effects of remote ischaemic preconditioning in patients undergoing coronary artery bypass surgery: a single-centre randomised, double-blind, controlled trial. Lancet 2013; 382(9892): 597-604.
16. Botker HE, Kharbanda R, Schmidt MR, et al. Remote ischaemic conditioning before hospital admission, as a complement to angioplasty, and effect on myocardial salvage in patients with acute myocardial infarction: a randomised trial. Lancet 2010; 375(9716): 727-34.
17. Heusch G. Cardioprotection: chances and challenges of its translation to the clinic. Lancet 2013; 381(9861): 166-75.
18. Ovize M, Thibault H, Przyklenk K. Myocardial conditioning: opportunities for clinical translation. Circulation research 2013; 113(4): 439-50.
19. Santos ES, Baltar VT, Pereira MP, et al. Comparison between cardiac troponin I and CK-MB mass in acute coronary syndrome without st elevation. Arquivos brasileiros de cardiologia 2011; 96(3): 179-87.
20. McErlean ES, Deluca SA, van Lente F, et al. Comparison of troponin T versus creatine kinase-MB in suspected acute coronary syndromes. The American journal of cardiology 2000; 85(4): 421-6.
21. Kannemeier C, Shibamiya A, Nakazawa F, et al. Extracellular RNA constitutes a natural procoagulant cofactor in blood coagulation. Proceedings of the National Academy of Sciences of the United States of America 2007; 104(15): 6388-93.

22. Deindl E, Fischer S, Preissner KT. New directions in inflammation and immunity: the multi-functional role of the extracellular RNA/RNase system. Indian journal of biochemistry & biophysics 2009; 46(6): 461-6.
23. Fischer S, Gerriets T, Wessels C, et al. Extracellular RNA mediates endothelial-cell permeability via vascular endothelial growth factor. Blood 2007; 110(7): 2457-65.
24. Fischer S, Grantzow T, Pagel JI, et al. Extracellular RNA promotes leukocyte recruitment in the vascular system by mobilising proinflammatory cytokines. Thrombosis and haemostasis 2012; 108(4): 730-41.
25. Cerri C, Chimenti D, Conti I, et al. Monocyte/macrophage-derived microparticles up-regulate inflammatory mediator synthesis by human airway epithelial cells. Journal of immunology 2006; 177(3): 1975-80.
26. Liehn EA, Piccinini AM, Koenen RR, et al. A new monocyte chemotactic protein-1/chemokine CC motif ligand-2 competitor limiting neointima formation and myocardial ischemia/reperfusion injury in mice. Journal of the American College of Cardiology 2010; 56(22): 1847-57.
27. Grohe C, van Eickels M, Wenzel S, et al. Sex-specific differences in ventricular expression and function of parathyroid hormone-related peptide. Cardiovascular research 2004; 61(2): 307-16.
28. Cabrera-Fuentes HA, Aslam M, Saffarzadeh M, et al. Internalization of Bacillus intermedius ribonuclease (BINASE) induces human alveolar adenocarcinoma cell death. Toxicon : official journal of the International Society on Toxinology 2013; 69: 219-26.
29. Inserte J, Barba I, Hernando V, et al. Delayed recovery of intracellular acidosis during reperfusion prevents calpain activation and determines protection in postconditioned myocardium. Cardiovascular research 2009; 81(1): 116-22.
30. Abassi ZA, Barac YD, Kostin S, et al. TVP1022 attenuates cardiac remodeling and kidney dysfunction in experimental volume overload-induced congestive heart failure. Circulation Heart failure 2011; 4(4): 463-73.
31. Rohman MS, Emoto N, Takeshima Y, et al. Decreased mAKAP, ryanodine receptor, and SERCA2a gene expression in mdx hearts. Biochemical and biophysical research communications 2003; 310(1): 228-35.
32. Simsekyilmaz S, Cabrera-Fuentes HA, Meiler S, et al. Role of extracellular RNA in atherosclerotic plaque formation in mice. Circulation 2014; 129(5): 598-606.
33. Acharya A, Baek ST, Huang G, et al. The bHLH transcription factor Tcf21 is required for lineage-specific EMT of cardiac fibroblast progenitors. Development 2012; 139(12): 2139-49.
34. Vorderwinkler KP, Mair J, Puschendorf B, et al. Cardiac troponin I increases in parallel to cardiac troponin T, creatine kinase and lactate dehydrogenase in effluents from isolated perfused rat hearts after hypoxia-reoxygenation-induced myocardial injury. Clinica chimica acta; international journal of clinical chemistry 1996; 251(1): 113-7.
35. Fischer S, Cabrera-Fuentes HA, Noll T, et al. Impact of extracellular RNA on endothelial barrier function. Cell and tissue research 2014.
36. Fischer S, Gesierich S, Griemert B, et al. Extracellular RNA liberates tumor necrosis factor-alpha to promote tumor cell trafficking and progression. Cancer research 2013; 73(16): 5080-9.
37. Gilles S, Zahler S, Welsch U, et al. Release of TNF-alpha during myocardial reperfusion depends on oxidative stress and is prevented by mast cell stabilizers. Cardiovascular research 2003; 60(3): 608-16.
38. Carpi A, Menabo R, Kaludercic N, et al. The cardioprotective effects elicited by p66(Shc) ablation demonstrate the crucial role of mitochondrial ROS formation in ischemia/reperfusion injury. Biochimica et biophysica acta 2009; 1787(7): 774-80.
39. Rodrigo R, Prieto JC, Castillo R. Cardioprotection against ischaemia/reperfusion by vitamins C and E plus n-3 fatty acids: molecular mechanisms and potential clinical applications. Clinical science 2013; 124(1): 1-15.
40. Bai Y, Muqier, Murakami H, et al. Cilostazol protects the heart against ischaemia reperfusion injury in a rabbit model of myocardial infarction: focus on adenosine, nitric oxide and mitochondrial

ATP-sensitive potassium channels. Clinical and experimental pharmacology & physiology 2011; 38(10): 658-65.
41. Bonner F, Borg N, Jacoby C, et al. Ecto-5'-nucleotidase on immune cells protects from adverse cardiac remodeling. Circulation research 2013; 113(3): 301-12.
42. Fischer S, Nishio M, Peters SC, et al. Signaling mechanism of extracellular RNA in endothelial cells. FASEB journal : official publication of the Federation of American Societies for Experimental Biology 2009; 23(7): 2100-9.
43. Fischer S, Preissner KT. Extracellular nucleic acids as novel alarm signals in the vascular system. Mediators of defence and disease. Hamostaseologie 2013; 33(1): 37-42.
44. Antoniak S, Boltzen U, Eisenreich A, et al. Regulation of cardiomyocyte full-length tissue factor expression and microparticle release under inflammatory conditions in vitro. Journal of thrombosis and haemostasis : JTH 2009; 7(5): 871-8.
45. Gedik N, Heusch G, Skyschally A. Infarct size reduction by cyclosporine A at reperfusion involves inhibition of the mitochondrial permeability transition pore but does not improve mitochondrial respiration. Archives of medical science : AMS 2013; 9(6): 968-75.
46. Kleinbongard P, Heusch G, Schulz R. TNFalpha in atherosclerosis, myocardial ischemia/reperfusion and heart failure. Pharmacology & therapeutics 2010; 127(3): 295-314.
47. Skyschally A, Gres P, Hoffmann S, et al. Bidirectional role of tumor necrosis factor-alpha in coronary microembolization: progressive contractile dysfunction versus delayed protection against infarction. Circulation research 2007; 100(1): 140-6.
48. Kleinbongard P, Schulz R, Heusch G. TNFalpha in myocardial ischemia/reperfusion, remodeling and heart failure. Heart failure reviews 2011; 16(1): 49-69.
49. Lecour S, Suleman N, Deuchar GA, et al. Pharmacological preconditioning with tumor necrosis factor-alpha activates signal transducer and activator of transcription-3 at reperfusion without involving classic prosurvival kinases (Akt and extracellular signal-regulated kinase). Circulation 2005; 112(25): 3911-8.

Acknowledgments

We thank Peter Volk, Baerbel Fuehler and Juri Schklarenko for their excellent technical assistance, Dr. Laureano de la Vega, Dr. Adrian Stachowicz and Dr. Barbara Griemert for helpful discussions. This work was supported in part by the German Research Council (DFG; Bonn, Germany) within the International Graduate School PROMISE (IRTG-1566, Giessen-Barcelona), the Excellence Cluster "Cardiopulmonary System" (ECCPS, Giessen), the DFG-Research Group "Chemokines and Adhesion Molecules in Cardiovascular Pathogenesis" (FOR 809), a University Hospital-Giessen-Marburg Cooperative Grant, as well as by the Interdisciplinary Centre for Clinical Research (IZKF; Aachen, Germany) and the University of Cape Town, South Africa. Dr. Ignasi Barba is a recipient of a Ramón y Cajal Fellowship (Barcelona, Spain). Dr. Derek J. Hausenloy is funded by a British Heart Foundation Senior Clinical Research Fellowship (FS/10/039/28270). This work was performed within the Russian Government Program of Competitive Growth of Kazan Federal University.

Conflict of Interest Statement

We declare that there are no financial or personal relationships with other people or organizations that can inappropriately influence our work, there is no professional or other personal interest of any nature or kind in any product, service and/or company that could be construed as influencing the position presented in, or the review of the manuscript.

Legends to Figures

Figure 1. Release of extracellular RNA during myocardial infarction following I/R. (**A**) Following induction of the *in vivo* cardiac I/R mice model with 60 min ischemia and 120 min reperfusion, plasma extracellular RNA was quantified at the indicated time points. Data represent mean ± SEM (n=6 mice per group; **P<0.01, ***P<0.001). (**B**) After coronary ligation for 60 min without reperfusion, the mRNAs of the following genes were quantified by real-time PCR to deduce their cellular origin: *Serca* (cardiomyocytes), α-*Sma* (smooth muscle cells), *Tcf21* (cardiac fibroblast), *Cd31* (endothelial cells), *Cd115* (macrophages), *Elane* (neutrophils) and *Mcpt6* (mast cells). Values are expressed as mean ±SEM (n=6); *P<0.05, **P<0.01, ***P<0.001 *vs GAPDH* expression. The insert indicates the electrophoretic mobility of 28S and 18S rRNA in a representative sample. (**C**) Isolated rat hearts (Langendorff-model) were submitted to I/R (45 min ischemia, followed by 120 min reperfusion), and extracellular RNA was quantified in the effluent fractions for each time point. Values are normalized to the effluent protein concentration and represent mean ± SD (n=9 hearts) as compared to the minimal values at 3-5 min; *P<0.05, **P<0.01, ***P<0.001. The insert indicates the microparticle-associated total RNA that was quantified from collected perfusate over 120 min and normalized to the effluent protein concentration. Values represent mean ± SD (n=9 hearts); **P<0.01.

Figure 2. Extracellular RNA potentiates the release of TNF-α under hypoxia. (**A**) After induction of the *in vivo* cardiac ischemia/reperfusion (I/R) mice model, sham-operated or coronary occluded animals with the following time intervals of I/R (in min): 60/0, 60/2 and 60/120, respectively, were left untreated (Buffer) or were treated with RNase1 (100 μg/mice) or RNase-inhibitor (RI, 80 U/mice) as indicated, and plasma TNF-α was quantified at the end of the respective experiment. Data represent mean ± SD (n=6-8 mice per group); *P<0.05,

P<0.01, ns=non-significant. (B**) Following induction of the *in vivo* cardiac I/R (60 min/120 min) mice model, the presence of TNF-α in cryosections from heart tissue was demonstrated by confocal microscopy. Representative merged images from immunofluorescence staining for TNF-α (red), F-actin (green) and nuclear DNA (DAPI, blue) are displayed. All images were obtained under identical conditions of confocal laser beam intensity and exposure time (n=6). (**C**) TNF-α-release was quantified in fractions throughout the first 15 min reperfusion period in the Langendorff heart, submitted to the I/R protocol as indicated. in the absence (squares) or presence of 10 μg/ml RNase1 (circles) or 2 U/ml RI (triangles). TNF-α values are corrected for the respective flow rate and normalized to the effluent protein concentration and represent mean ± SD (n=3-6 hearts); $^{\#}$P<0.001 (I/R *vs.* pre-ischemic values); *P<0.001 (I/R+RNase1 *vs.* I/R).

Figure 3. Prevention of ROS production by RNase1. (**A**) After induction of the *in vivo* cardiac I/R mice model, sham-operated or coronary occluded animals with the following time intervals of I/R (in min): 60/0, 60/2 and 60/120, respectively, were left untreated (Buffer) or were treated with RNase1 (100 μg/mice) or RNase-inhibitor (RI, 80 U/mice) as indicated. (**B**) Isolated Langendorff-perfused hearts were either submitted to 3h perfusion under normoxia (sham) or exposed to the I/R protocol with the following time intervals of I/R (in min): 45/0, 45/2, 45/120, in the absence (Buffer) or in the presence of RNase1 (10 μg/ml) or RI (2 U/ml) as indicated. The distribution of ROS (dihydroethidium, red) production together with detection of F-actin (green) and nuclear DNA (DAPI, blue) was quantified by immunofluorescent staining in microslices of cardiac tissue in each case. All samples received the same manipulation and all images were obtained under identical conditions of laser beam intensity and exposure time using confocal microscopy. Values represent mean ± SD (n=6-8 per group); *P<0.05, **P<0.01, ***P<0.001. Representative images of multiple experiments are shown.

Figure 4. Extracellular RNA-induced cell death during ischemia: prevention by RNase1 treatment. (**A**) Following the induction of the *in vivo* acute cardiac I/R mice model, infarct size in mice hearts was quantified after coronary occlusion followed by 2h reperfusion in the absence (Buffer) or presence of RNase1 (100 μg/mice) or RNase-inhibitor (RI, 80 U/mice), respectively. Representative pictures show myocardial infarct size in heart sections indicated by dual staining with 2,3,5-triphenyltetrazolium (TTC) and Evans blue. Data represent mean ± SEM (n=6-8 mice per group; **P<0.01, ***P<0.001, ns=non-significant). (**B**) Following the induction of the *in vivo* long-term cardiac I/R mice model, histo-morphological analysis was used to evaluate infarct size in mice hearts in the absence (without I/R) or presence (I/R) of coronary occlusion followed by 14 days of reperfusion. In comparison to sham-operated animals, the other groups were continuously treated with buffer only or with RNase1 (100 μg/mice) or RNase-inhibitor (RI, 80 U/mice), respectively, by infusion via subcutaneously implanted osmotic pump. Representative pictures show myocardial infarct size in heart sections indicated by Gomori 1-step stain. Data represent mean ± SEM (n=6-8 mice per group; *P<0.05, ***P<0.001, ns=non-significant). (**C**) Isolated rat hearts (Langendorff-model) were submitted to perfusion only under normoxia (sham) or submitted to I/R (45 min/120 min) in the absence (Buffer) or presence of 10 μg/ml RNase1 or 2 U/ml RI, respectively. Release of lactate dehydrogenase (LDH) during 120 min reperfusion was measured in the absence (Buffer) or presence of different doses of RNase1 or RI (2 U/ml) as indicated. LDH activity was quantified for each time point and normalized to the tissue weight. Values represent mean ± SEM (n=6-9 hearts); *P<0.05, **P<0.01, ***P<0.001. **(D)** Based on the aforementioned experimental conditions; infarct size in the isolated rat heart model was quantified by the TTC reaction in heart sections and expressed as the percentage of necrotic tissue with respect to total ventricular mass in the different treatment groups indicated. Values represent mean ± SD (n=6-9 hearts); **P<0.01, ***P<0.001, ns=non-significant.

Figure 1

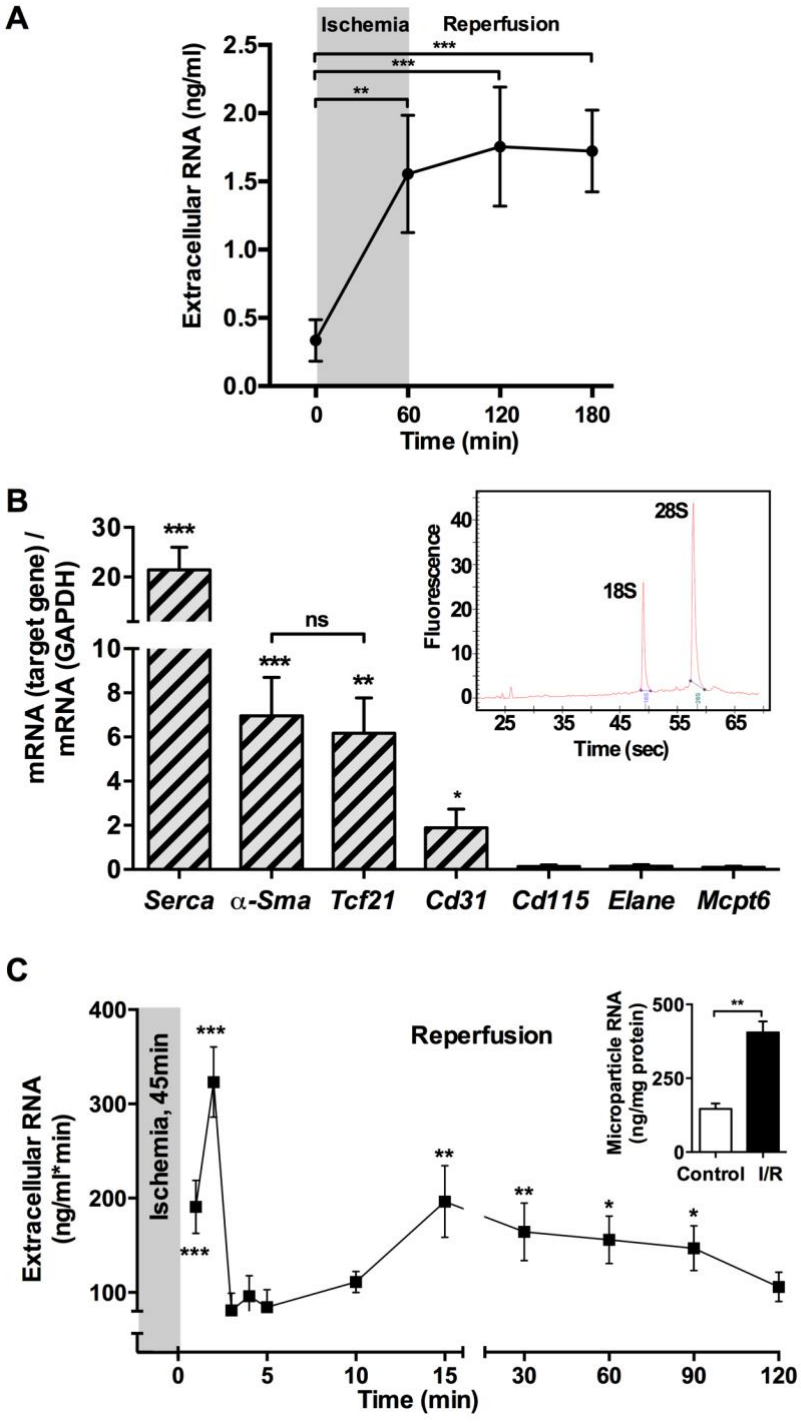
A
Ischemia
Reperfusion
Extracellular RNA (ng/ml)
Time (min)
B
mRNA (target gene) / mRNA (GAPDH)
ns
Fluorescence
28S
18S
Time (sec)
Serca
α-Sma
Tcf21
Cd31
Cd115
Elane
Mcpt6
C
Extracellular RNA (ng/ml*min)
Ischemia, 45min
Reperfusion
Microparticle RNA (ng/mg protein)
Control
I/R
Time (min)

Figure 2

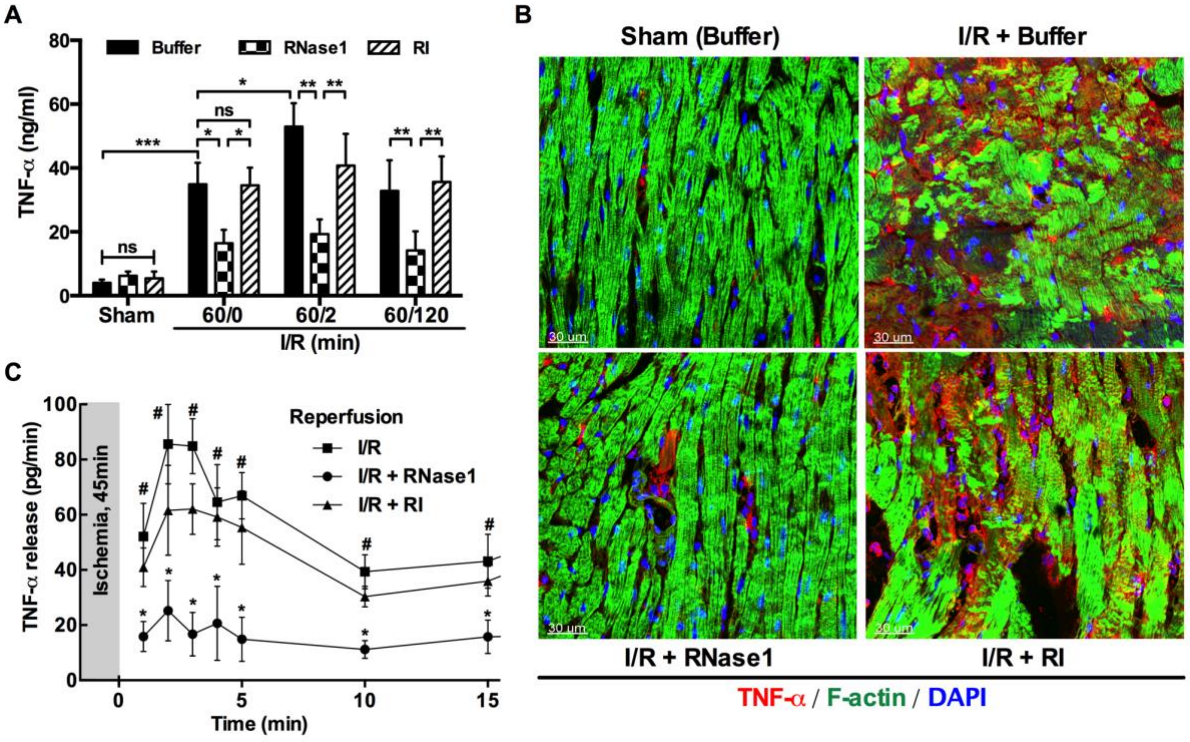
A
Buffer
RNase1
RI
TNF-α (ng/ml)
Sham
60/0
60/2
60/120
I/R (min)
B
Sham (Buffer)
I/R + Buffer
I/R + RNase1
I/R + RI
TNF-α / F-actin / DAPI
C
Reperfusion
I/R
I/R + RNase1
I/R + RI
Ischemia, 45min
TNF-α release (pg/min)
Time (min)

Figure 3

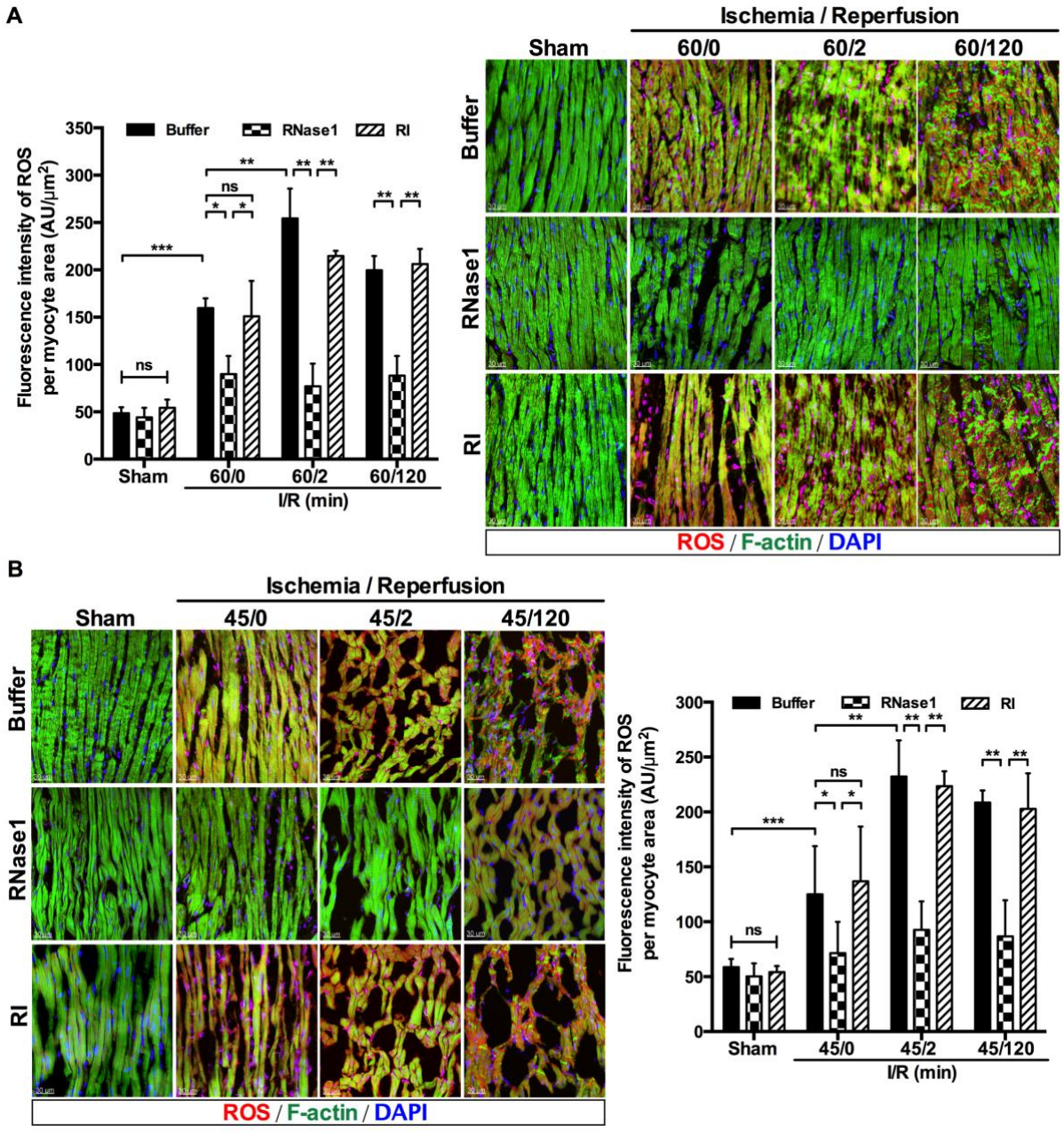
A
Ischemia / Reperfusion
Sham
60/0
60/2
60/120
Buffer
RNase1
RI
Buffer
RNase1
RI
Fluorescence intensity of ROS per myocyte area (AU/μm²)
Sham
60/0
60/2
60/120
I/R (min)
ROS / F-actin / DAPI
B
Ischemia / Reperfusion
Sham
45/0
45/2
45/120
Buffer
RNase1
RI
Buffer
RNase1
RI
Fluorescence intensity of ROS per myocyte area (AU/μm²)
Sham
45/0
45/2
45/120
I/R (min)
ROS / F-actin / DAPI

Figure 4

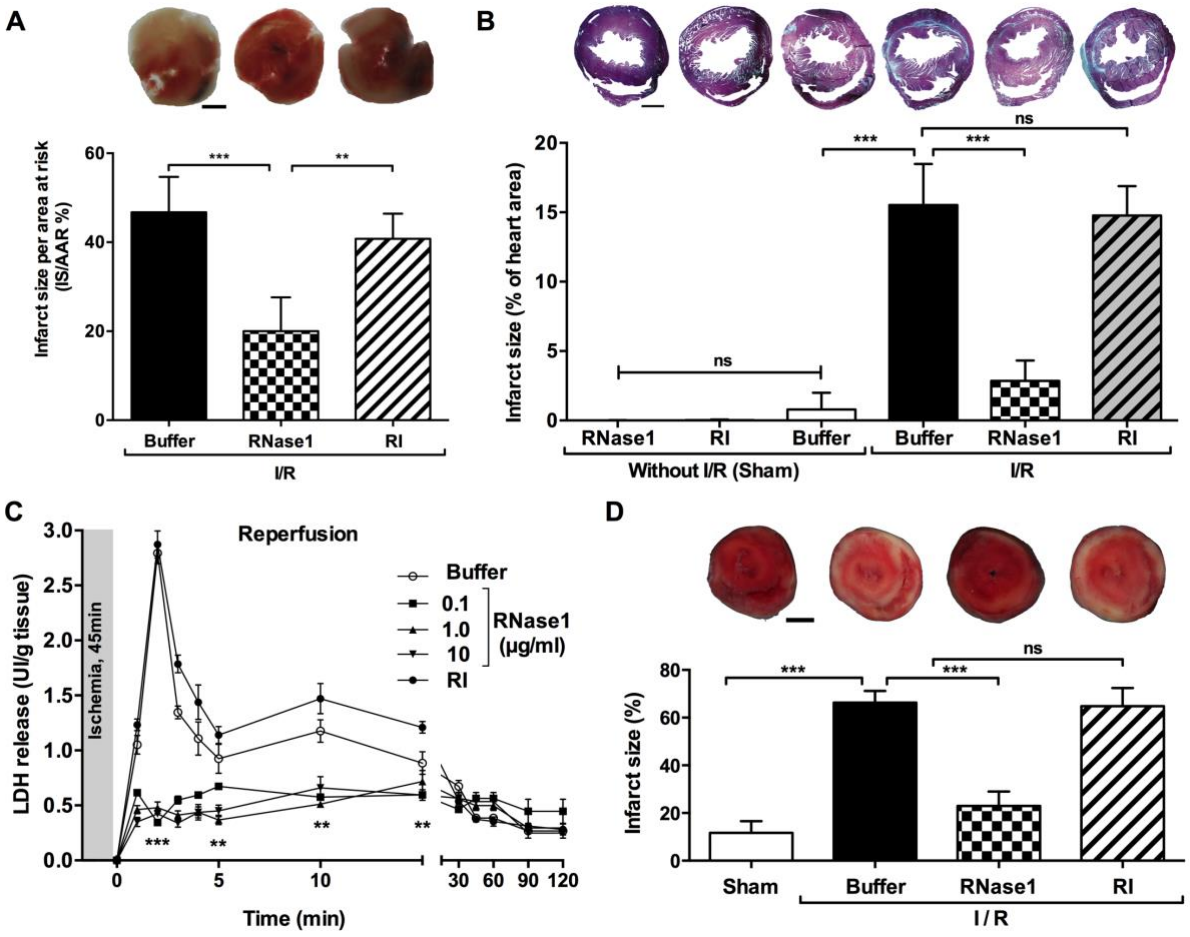
A
Infarct size per area at risk (IS/AAR %)
Buffer
RNase1
RI
I/R
B
Infarct size (% of heart area)
ns
RNase1
RI
Buffer
Without I/R (Sham)
I/R
C
Reperfusion
Ischemia, 45min
LDH release (UI/g tissue)
Buffer
0.1
1.0
10
RI
RNase1 (µg/ml)
Time (min)
D
Infarct size (%)
Sham
Buffer
RNase1
RI
I / R